A facile method for precise layer number identification of two-dimensional materials through optical images

Jiayu Lei[a], Jiafan Qu[a], Peng Wang[a], Hu Jiang[a], Hongyan Shi[a, b], Xiudong Sun[a, b], and Bo Gao[a, b, *]

[a] Institute of Modern Optics, Department of Physics, Key Laboratory of Micro-Nano Optoelectronic Information System, Ministry of Industry and Information Technology, Key Laboratory of Micro-Optics and Photonic Technology of Heilongjiang Province, Harbin Institute of Technology, Harbin 150001, China

[b] Collaborative Innovation Center of Extreme Optics, Shanxi University, Taiyuan 030006, China

Abstract

Optical microscopy is believed to be an efficient method for identifying layer number of two-dimensional (2D) materials. However, since illuminants, cameras and their parameters are different from lab to lab, it is impossible to identify layer numbers merely by comparing a given optical image with standard or calculated images under standard conditions. Here we reported an image reconstruction method, converting raw optical images acquired by arbitrary illuminants and cameras into reconstructed images under the condition of specified illuminant and specified camera. After image reconstruction, the color differences of each layer number roughly equaled those calculated under the specified condition. By comparing the color differences in the reconstructed image with those calculated under the specified condition, the layer numbers of 2D materials in our lab and published papers, including MoS_2, WS_2, and WSe_2, were unambiguously identified. This study makes optical microscopy a precise method to identify layer numbers of 2D materials on known substrates.

[*] Corresponding author. E-mail: gaobo@hit.edu.cn

Keywords: 2D materials; Layer number; Optical microscopy, Image processing

1. Introduction

Since the discovery of monolayer graphene in 2004, various two-dimensional (2D) materials, such as hexagonal boron nitride (h-BN), transition metal dichalcogenides (TMDs) and black phosphorus (BP), have attracted remarkable interest due to potential applications in thin-film electronics and optoelectronics. Generally, physical properties of 2D materials are closely correlated with their electronic structures, which are greatly influenced by their layer numbers [1-4]. Experimentally, atomic force microscopy (AFM) [5, 6] and Raman spectroscopy [7, 8] are the most common methods for layer number identification. Despite of high reliability, these methods require time-consuming procedures and operations for large scale 2D materials. A lot of efforts have been made to develop new methods to fulfill both reliability and efficiency. Therein, optical microscopy is believed to be a suitable method. Based on the interference theory, the optical contrast between a substrate (usually a SiO_2/Si substrate with known oxide thickness) and 2D material is considered to be a function of layer numbers, which can be utilized to identify layer numbers [9-12].

The optical contrast distribution is actually a grayscale image with a range from zero to one, while an optical RGB image retains additional degrees of spectral information. To achieve more precise results, all the channels of an image are supposed to be taken into account. So far, color differences in CIELab color space [13], sRGB color space [14-17] and CIE XYZ color space [18] have been calculated to quantitatively analyze layer

numbers of 2D materials.

The optical image of 2D materials is mainly influenced by the reflectance of the object calculated with corresponding refractive index [19], the spectrum of the illuminant, the camera and its setups (such as white balance and exposure). However, as illuminants and cameras are different from lab to lab, it is impossible to identify layer numbers by comparing with published images. Therefore, although theoretically feasible, optical microscopy has never been an independent layer number identification method for 2D materials, and the calculation results of most optical images cannot be directly compared between different published works so far [20].

In this study, we converted raw optical images acquired by arbitrary illuminants and cameras to new images under the condition of specified illuminant and specified camera by image reconstruction. After image reconstruction, the color differences roughly equaled those calculated under the specified condition for specific 2D materials on known substrates, regardless of illuminant or camera. This method, bypassing the illuminants and cameras, provides a precise tool to identify layer numbers of thin 2D materials.

2. Color difference and image reconstruction

The color of an image is usually studied in a color space, e.g. CIE (International Commission on Illumination) XYZ color space, where a certain color is described in a three-dimensional coordinate. By CIE color-matching equations, the color of an object in CIE XYZ color space is given as follows [21]:

$$
\begin{aligned}
X &= k\int_{380\ \mathrm{nm}}^{780\ \mathrm{nm}} R(\lambda)I(\lambda)\,\bar{x}(\lambda)d\lambda \\
Y &= k\int_{380\ \mathrm{nm}}^{780\ \mathrm{nm}} R(\lambda)I(\lambda)\,\bar{y}(\lambda)d\lambda \\
Z &= k\int_{380\ \mathrm{nm}}^{780\ \mathrm{nm}} R(\lambda)I(\lambda)\,\bar{z}(\lambda)d\lambda \\
k &= \frac{100}{\int_{380\ \mathrm{nm}}^{780\ \mathrm{nm}} I(\lambda)\bar{y}(\lambda)d\lambda}
\end{aligned}
\tag{1}
$$

where X, Y, and Z are tristimulus values which describe the color of an object (such as 2D materials nanosheets) in CIE XYZ color space. k is the normalization coefficient. $R(\lambda)$ is the spectral reflectance of the object. $I(\lambda)$ is the spectral power distribution (SPD) of the illuminant. $\bar{x}(\lambda)$, $\bar{y}(\lambda)$ and $\bar{z}(\lambda)$ are the color matching functions of the camera or the observer.

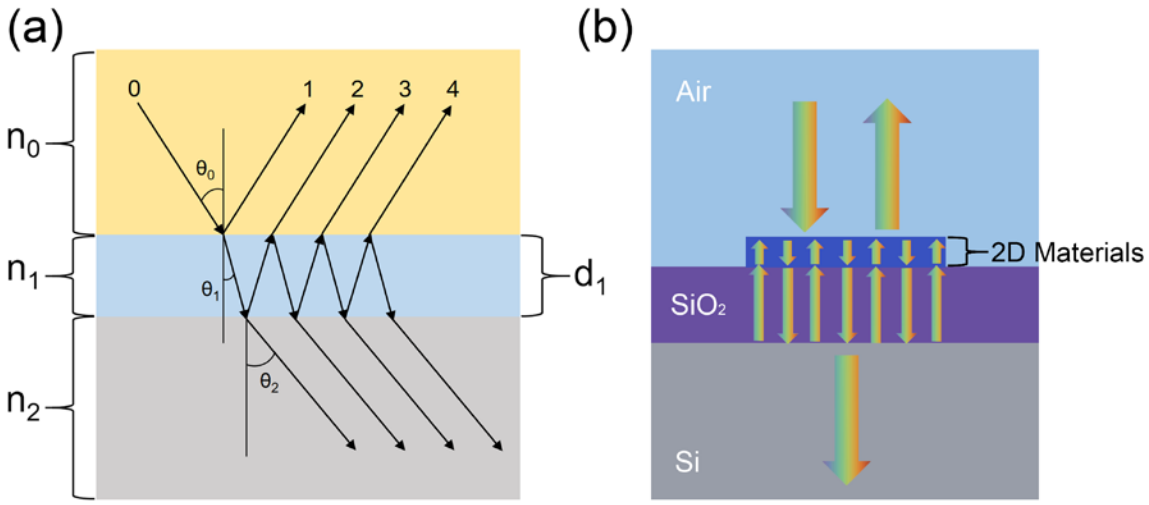

Fig. 1. (a) Diagram of thin-film interference model. (b) Optical reflection and transmission schematic for a layered 2D material nanosheet on SiO_2/Si substrate.

$R(\lambda)$ is related to thin-film interference in this model. Fig. 1(a) is a diagram of thin-film interference model, where incident light with incident angles θ_0 reflects over the interface between the incident medium and a thin-film object. Fig. 1(b) illustrates the real condition in experiment. The substrate with refractive index n_2 is assumed to be semi-

infinite (no light reflects from the substrate). In Fig. 1(a), n and d refer to refractive index and thickness of media, respectively, while subscript i (=0, 1, 2 ….) is the number of film. The relative amplitude of the system with two interfaces is shown in Eq. (2) [9, 22], where δ_i is the phase shift due to changes in the optical path as it travels through i numbered film, and r_{ij} is a relative index.

$$r = \frac{E_R}{E_0} = \frac{r_{01}+r_{12}e^{-2i\delta_1}}{1+r_{01}r_{12}e^{-2i\delta_1}}, \text{ where}$$

$$\delta_i = \frac{2\pi}{\lambda} n_i d_i \cos\theta_i,\ r_{ij} = \frac{n_i \cos\theta_i - n_j \cos\theta_j}{n_i \cos\theta_i + n_j \cos\theta_j},\ i,j = 0,1,2 \ldots \quad (2)$$

Using the described two interfaces thin-film interference model, recurrence relation of multilayer thin-film interference model is shown in Eq. (3) [9, 22]

$$r_1 = \frac{r_{01} + r_{12}e^{-2i\delta_1}}{1 + r_{01}r_{12}e^{-2i\delta_1}} \quad r_2 = \frac{r_1 + r_{23}e^{-2i\delta_2}}{1 + r_1 r_{23}e^{-2i\delta_2}} \quad r_3 = \frac{r_2 + r_{34}e^{-2i\delta_3}}{1 + r_2 r_{34}e^{-2i\delta_3}} \quad \ldots$$

$$R = r_{Final} \cdot r^*_{Final} = |r_{Final}|^2 \quad (3)$$

where R is reflectance of the system. Since refractive indices are wavelength dependent, R can be written as $R(\lambda)$ in Eq. (1). It is worth noting that Eq. (3) is applied only to normal incidence situation, which indicates as $\theta_i = 0$. However, in an experimental optical microscope system with a finite numerical aperture, the intensity of such incident light on the sample follows the Normal Distribution along the angle of incidence. Even $\theta_i = 0$ is not a perfect hypothesis, due to the Normal Distribution of incident and reflected light for different angles, such influence can be neglected [13].

Then, by Eq. (1), the color difference between substrate and 2D materials can be expressed as $\Delta E_{XYZ} = \sqrt{(X_{2D} - X_s)^2 + (Y_{2D} - Y_s)^2 + (Z_{2D} - Z_s)^2}$, where

(X_{2D}, Y_{2D}, Z_{2D}) and (X_s, Y_s, Z_s) are color coordinates of 2D materials and substrates, respectively. Since CIELab color space with CIE76 definition is designed to be more perceptually uniform to human color vision than CIE XYZ color space, the color difference between a substrate and a 2D material nanosheet is usually defined as

$$\Delta E_{ab}^{*} = \sqrt{(L_{2D} - L_s)^2 + (a_{2D} - a_s)^2 + (b_{2D} - b_s)^2} \quad (4)$$

where (L_{2D}, a_{2D}, b_{2D}) and (L_s, a_s, b_s) are color coordinates of 2D materials and substrates in CIELab color space, respectively. Thus, if SPD, color matching functions and oxide thickness of the substrate are known, we can directly obtain the layer number from ΔE_{ab}^{*}.

In practice, parameters such as SPD and color matching functions about optical microscopy are usually undefined. So we manage to convert a raw image under an arbitrary condition to a new image under a specified condition. To achieve larger color differences, we specify CIE Standard Illuminant A [23] as the illuminant and CIE standard observer [23] as the camera, which are defined as the specified condition in this work (See Fig. S1 for calculated color image under the specified condition and other conditions in Supplementary Material).

For a 2D nanosheet on SiO_2/Si substrate with known oxide thickness, the reflectance spectrum and hence the color of the substrate are fixed under a specified condition. So the color of a substrate can be referred to reconstruct the raw image under arbitrary conditions.

The color of each pixel in an image can be expressed as a three elements' vector. For simplicity, we reformulated Eq. (1) in terms of a matrix product:

$$\mathbf{t} = \mathbf{ALr} \tag{5}$$

where $\mathbf{t} = [X\ Y\ Z]^T$ contains tristimulus values, the columns of the $3 \times N$ matrix $\mathbf{A}$ include the CIE XYZ color matching functions; $\mathbf{L}$ is an diagonal matrix whose diagonal elements are the spectral power distribution; N elements' vector $\mathbf{r}$ is the spectral reflectance of an object. Therefore, XYZ tristimulus values under the specified condition are

$$\mathbf{t}_{spe} = \mathbf{A}_{spe}\mathbf{L}_{spe}\mathbf{r} \tag{6}$$

For a raw image with arbitrary illuminant and color matching functions, tristimulus values are

$$\mathbf{t}_{raw} = \mathbf{A}_{raw}\mathbf{L}_{raw}\mathbf{r} \tag{7}$$

As mentioned above, the substrate's color under the specified condition is regarded as the reference. Then, by utilizing XYZ tristimulus values' differences of the substrate between the specified condition and the raw image, we can reconstruct the whole raw image and obtain XYZ tristimulus values of a reconstructed image by Eq. (8) [24]:

$$\mathbf{t}_{rec} = \mathbf{t}_{raw} + \alpha J\left(\mathbf{t}_{spesub} - \mathbf{t}_{rawsub}\right) \tag{8}$$

where $\mathbf{t}_{spesub}$ and $\mathbf{t}_{rawsub}$ represent XYZ tristimulus values of substrate under the specified condition and in the raw image; $\mathbf{t}_{raw}$ is the tristimulus values of 2D materials in raw image; $\mathbf{t}_{rec}$ is the tristimulus values of reconstructed image; αJ is a nonlinear transformation. In this work, $\alpha J = 1$ is used, as we do not know the exact relationship between color and layer number in a raw image.

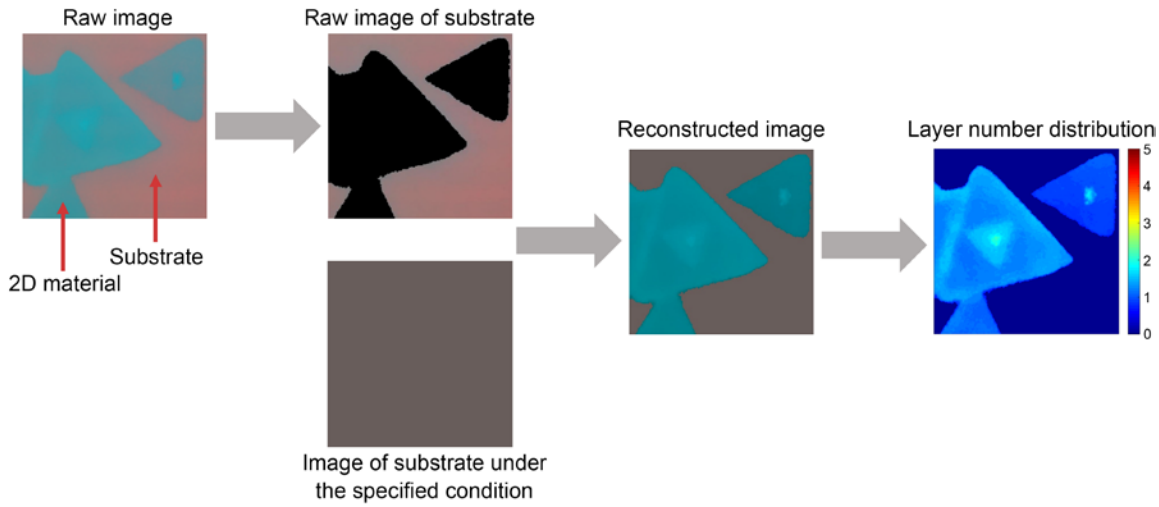

Fig. 2. Procedures of image reconstruction and layer number distribution calculation.

Based on the method above, the optical image reconstruction and layer number distribution calculation procedures are shown in Fig. 2. Firstly, we choose the substrate domain in a raw image and then calculate the average sRGB values of the substrate, which are subsequently converted to XYZ tristimulus values.

After calculating XYZ tristimulus values of the substrate under the specified condition, we get XYZ tristimulus values' differences of the substrate between the specified condition and the raw image. Then, the XYZ tristimulus values' differences are applied to each pixel of the raw image based on Eq. (8), so that we can obtain the XYZ tristimulus values of the reconstructed image.

In the end, the obtained tristimulus values of the whole image are converted back to sRGB values for display and CIELab values for layer number distribution calculation. Based on Eq. (1) and Eq. (4) to calculate the color difference relationship between substrate and nanosheets under the specified condition, the layer number of each pixel, and in a larger

scale, each domain can be finally identified. (See step-by-step details about the whole procedure and codes in Supplementary Material)

3. Layer number identification from reconstructed calculated image

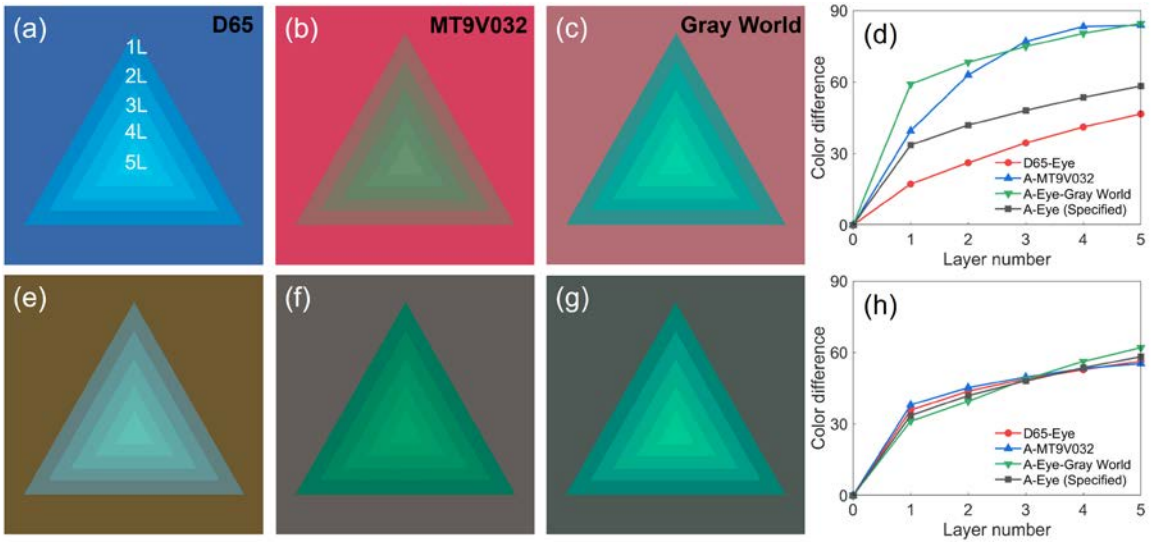

Fig. 3. Calculated optical images of MoS_2 nanosheets consisting of 1-5 layers on SiO_2/Si substrate, with illuminant D65 and CIE standard observer (a) before (e) after image reconstruction; with illuminant A and EO-0413C Camera with uEye MT9V032 CMOS (Edmund Optics) (b) before (f) after image reconstruction; with illuminant A and CIE standard observer, and Gray World AWB algorithm calibration (c) before (g) after image reconstruction. Color differences between MoS_2 nanosheets and SiO_2/Si substrate versus layer numbers (d) before (h) after image reconstruction.

To demonstrate the feasibility, we calculated three optical images of MoS_2 nanosheets consisting of 1-5 layers on Si substrate with 300 nm SiO_2 layer (SiO_2/Si) under three selected conditions and then reconstructed the three images. In Fig. 3(a) we used Illuminant D65 [23] as the illuminant. In Fig. 3(b) we used MT9V032 [25] CMOS as the camera. In

Fig. 3(c) we used Gray World algorithm [26] for white balance calibration. It can be seen that there are different contrasts between the substrate and nanosheets with different layer numbers in all three images. Fig. 3(d) shows the color differences versus layer numbers extracted from the three images (color difference values are shown in Table SI in Supplementary Material) and the image under the specified condition (See Fig. S1(a) in Supplementary Material). It can be seen that the color differences are increasing with layer numbers, which indicates that layer number can be identified by color difference. However, it is noted that there are remarkable differences between color differences of each layer number in the four images. Therefore, it is highly possible to inaccurately identify layer numbers by comparing color differences extracted from optical images acquired under different conditions.

Fig. 3(e), (f) and (g) show the reconstructed images from Fig. 3(a), (b) and (c), respectively. Fig. 3(h) shows the color differences versus layer numbers extracted from the three reconstructed images and the image under the specified condition (color difference values are shown in Table SI in Supplementary Material). It can be seen that the color differences extracted from the reconstructed images are roughly equal to those extracted from the image under the specified condition. More examples under different conditions are shown in Fig. S2 (See Supplementary Material). Therefore, after image reconstruction, we can accurately identify layer numbers by comparing color differences extracted from reconstructed images.

4. Layer number identification from reconstructed experimental image

To testify to the universality of the image reconstruction method, we reconstructed some optical images of 2D materials in our lab and in published papers. Fig. 4(a) and (b) show the raw and reconstructed optical images of our CVD-grown MoS_2 nanosheets sample on Si substrate with 300 nm thick SiO_2 layer. Optical images were obtained by an EO-0413C camera (Edmund Optics) with uEye MT9V032 CMOS attached to an Olympus BX51 optical microscope under Olympus U-LH100-3 halogen illuminant. Raman measurement shows that there are monolayer, bilayer, and trilayer MoS_2 nanosheets (See Fig. S3 in Supplementary Material), as indicated in Fig. 4(a).

The purple curves and black curves in Fig. 4(c) show the color differences versus layer numbers extracted from Fig. 4(a) and Fig. S1(a), respectively (color difference values are shown in Table SII in Supplementary Material). It can be seen that color differences are increasing with layer numbers, while there are remarkable differences between color differences of each layer number under the experimental condition and the specified condition (e.g., color differences of monolayer MoS_2 in Fig. 4(a) and Fig. S1(a) are 55.4 and 33.6). After reconstruction, as shown in Fig. 4(d), all the color differences of each layer number in reconstructed optical image roughly equal those under the specified condition (e.g., color differences of monolayer MoS_2 is 36.6, close to 33.6). We also reconstructed three published optical images of MoS_2 on Si substrate with 300 nm SiO_2 layer (see reconstructed images in Fig. S4 in Supplementary Material), and plotted the color differences versus layer numbers for raw image and reconstructed image in Fig. 4(c) and (d), respectively. For raw images, the color differences of each layer number have a broad

range (e.g., for monolayer, color differences range from 16.3 to 43.1). After image reconstruction, all the color differences of each layer number are roughly equal to those under the specified condition (e.g., for monolayer, color differences range from 32.5 to 34.0, close to 33.6). Therefore, we can identify layer numbers of MoS_2 nanosheets merely from reconstructed optical images, even though the illuminants and cameras are unknown.

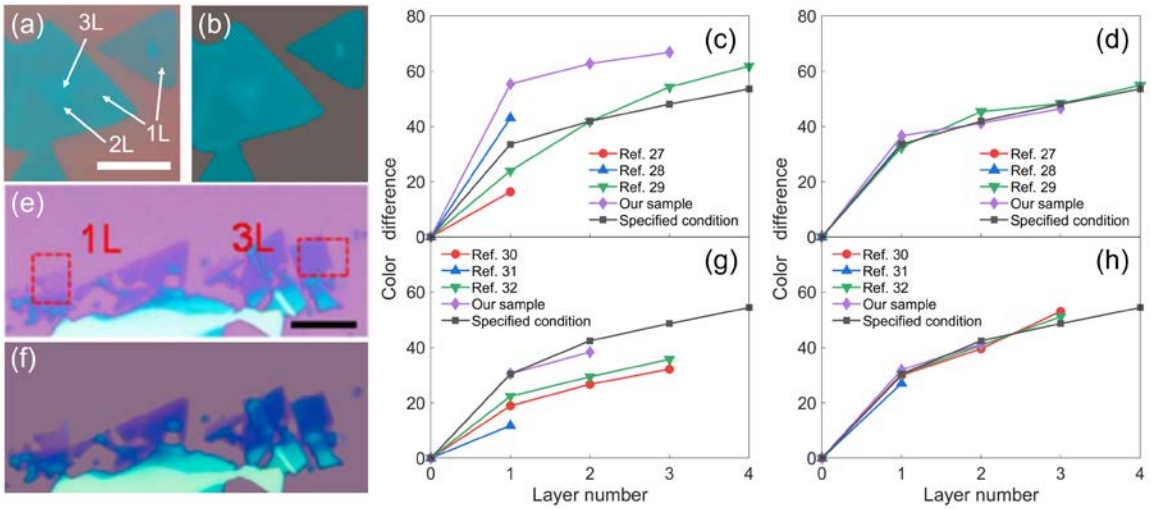

Fig. 4. Optical images of our MoS_2 sample (a) before (b) after image reconstruction, and color differences between MoS_2 nanosheets [27-29] and SiO_2/Si substrate versus layer numbers (c) before (d) after image reconstruction. Scale bar: 25 μm. Optical images of WS_2 nanosheets [30] (e) before (f) after image reconstruction, and color differences between WS_2 nanosheets [30-32] and SiO_2/Si substrate versus layer numbers (g) before (h) after image reconstruction. Scale bar: 5 μm.

We also applied the image reconstruction method to other 2D materials. Fig. 4(e) and (f) show the raw and reconstructed optical images of WS_2 nanosheets on Si substrate with 300 nm thick SiO_2 layer [30]. Fig. 4(g) and (h) show the color differences in raw image

and reconstructed image versus layer numbers for WS_2 nanosheets in our lab and in published papers [30-32] (See raw and reconstructed images in Fig. S4 and color difference values in Table SIII in Supplementary Material). For raw images, the color differences of each layer number of WS_2 have broad ranges due to different illuminants and cameras. After image reconstruction, all the color differences of each layer number are very close to those under the specified condition. Similar results are also found in WSe_2 nanosheets [10, 33] (See Fig. S5 in Supplementary Material). Therefore, optical microscopy can be a precise independent method for identifying layer numbers of various 2D materials through image reconstruction.

5. Conclusion

In this work, we develop an image reconstruction method to identify layer numbers of 2D materials through image reconstruction. With our method, raw optical images acquired by arbitrary illuminants and cameras were reconstructed into new images under the condition of the specified illuminant and camera. After image reconstruction, the color differences of each layer number were getting close to those calculated under the specified condition. By comparing the color differences in the reconstructed image with those calculated under the specified condition, the layer numbers of 2D materials in our lab and published papers, including MoS_2, WS_2, and WSe_2, were unambiguously identified. This study makes optical microscope a precise method for identifying layer numbers of 2D materials on known substrates.

Acknowledgments

We appreciate Yuege Xie (the University of Texas at Austin) for helpful discussions. This study is financially supported by the National Natural Science Foundation of China (No. 21473046) and the New Faculty Start-up Funds from Harbin Institute of Technology.

References

[1] J. Zheng, X. Yan, Z. Lu, H. Qiu, G. Xu, X. Zhou, P. Wang, X. Pan, K. Liu, L. Jiao, High-Mobility Multilayered MoS_2 Flakes with Low Contact Resistance Grown by Chemical Vapor Deposition, Adv. Mater. , 29 (2017).
[2] A. Splendiani, L. Sun, Y. Zhang, T. Li, J. Kim, C.Y. Chim, G. Galli, F. Wang, Emerging photoluminescence in monolayer MoS_2, Nano Lett. , 10 (2010) 1271-1275.
[3] K.F. Mak, M.Y. Sfeir, J.A. Misewich, T.F. Heinz, The evolution of electronic structure in few-layer graphene revealed by optical spectroscopy, Proc. Natl. Acad. Sci. USA, 107 (2010) 14999-15004.
[4] X. Ling, H. Wang, S. Huang, F. Xia, M.S. Dresselhaus, The renaissance of black phosphorus, Proc. Natl. Acad. Sci. USA, 112 (2015) 4523-4530.
[5] K.S. Novoselov, D. Jiang, F. Schedin, T.J. Booth, V.V. Khotkevich, S.V. Morozov, A.K. Geim, Two-dimensional atomic crystals, Proc. Natl. Acad. Sci. USA, 102 (2005) 10451-10453.
[6] K.S. Novoselov, A.K. Geim, S.V. Morozov, D. Jiang, Y. Zhang, S.V. Dubonos, I.V. Grigorieva, A.A. Firsov, Electric field effect in atomically thin carbon films, Science, 306 (2004) 666-669.
[7] X. Li, W. Cai, J. An, S. Kim, J. Nah, D. Yang, R. Piner, A. Velamakanni, I. Jung, E. Tutuc, S.K. Banerjee, L. Colombo, R.S. Ruoff, Large-area synthesis of high-quality and uniform graphene films on copper foils, Science, 324 (2009) 1312-1314.
[8] R. Saito, Y. Tatsumi, S. Huang, X. Ling, M.S. Dresselhaus, Raman spectroscopy of transition metal dichalcogenides, J Phys Condens Matter, 28 (2016) 353002.
[9] P. Blake, E.W. Hill, A.H. Castro Neto, K.S. Novoselov, D. Jiang, R. Yang, T.J. Booth, A.K. Geim, Making graphene visible, Appl. Phys. Lett. , 91 (2007) 063124.
[10] M.M. Benameur, B. Radisavljevic, J.S. Heron, S. Sahoo, H. Berger, A. Kis, Visibility of dichalcogenide nanolayers, Nanotechnology, 22 (2011) 125706.
[11] Z.H. Ni, H.M. Wang, J. Kasim, H.M. Fan, T. Yu, Y.H. Wu, Y.P. Feng, Z.X. Shen, Graphene thickness determination using reflection and contrast spectroscopy, Nano Lett. , 7 (2007) 2758-2763.
[12] D. Golla, K. Chattrakun, K. Watanabe, T. Taniguchi, B.J. LeRoy, A. Sandhu, Optical thickness determination of hexagonal boron nitride flakes, Appl. Phys. Lett. , 102 (2013) 161906.

[13] L. Gao, W. Ren, F. Li, H.M. Cheng, Total color difference for rapid and accurate identification of graphene, ACS Nano, 2 (2008) 1625-1633.
[14] S.F.A. Rahman, A.M. Hashim, S. Kasai, Identification of Graphene Layer Numbers from Color Combination Contrast Image for Wide-Area Characterization, Japanese Journal of Applied Physics, 51 (2012) 06FD09.
[15] H. Li, J. Wu, X. Huang, G. Lu, J. Yang, X. Lu, Q. Xiong, H. Zhang, Rapid and reliable thickness identification of two-dimensional nanosheets using optical microscopy, ACS Nano, 7 (2013) 10344-10353.
[16] J. Lee, S. Cho, S. Park, H. Bae, M. Noh, B. Kim, C. In, S. Yang, S. Lee, S.Y. Seo, J. Kim, C.-H. Lee, W.-Y. Shim, M.-H. Jo, D. Kim, H. Choi, Highly efficient computer algorithm for identifying layer thickness of atomically thin 2D materials, J. Phys. D: Appl. Phys. , 51 (2018) 11LT03.
[17] B.S. Jessen, P.R. Whelan, D.M.A. Mackenzie, B. Luo, J.D. Thomsen, L. Gammelgaard, T.J. Booth, P. Boggild, Quantitative optical mapping of two-dimensional materials, Sci Rep, 8 (2018) 6381.
[18] Y.-F. Chen, D. Liu, Z.-G. Wang, P.-J. Li, X. Hao, K. Cheng, Y. Fu, L.-X. Huang, X.-Z. Liu, W.-L. Zhang, Y.-R. Li, Rapid Determination of the Thickness of Graphene Using the Ratio of Color Difference, The Journal of Physical Chemistry C, 115 (2011) 6690-6693.
[19] Y. Li, A. Chernikov, X. Zhang, A. Rigosi, H.M. Hill, A.M. van der Zande, D.A. Chenet, E.-M. Shih, J. Hone, T.F. Heinz, Measurement of the optical dielectric function of monolayer transition-metal dichalcogenides: MoS_2, $MoSe_2$, WS_2, and WSe_2, Phys. Rev. B, 90 (2014).
[20] D. Bing, Y. Wang, J. Bai, R. Du, G. Wu, L. Liu, Optical contrast for identifying the thickness of two-dimensional materials, Optics Communications, 406 (2018) 128-138.
[21] J. Schanda, Colorimetry: Understanding the CIE System, John Wiley & Sons2007.
[22] M. Born, E. Wolf, Principles of Optics, 7th (expanded) ed, Cambridge U. Press, Cambridge, UK1999.
[23] C.I.d. l'Eclairage, Colorimetry: Technical Report, Central Bureau of the CIE2004.
[24] M.J. Vrhel, H.J. Trussell, Color device calibration: a mathematical formulation, IEEE Trans. Image Process. , 8 (1999) 1796-1806.
[25] http://www.ids-imaging.com/go/edmund/ for "Color Matching Functions Data of Edmund Optics-0413C Camera with uEye MT9V032 CMOS" (last accessed: April 2018).
[26] M. Ebner, Color constancy, John Wiley & Sons2007.
[27] N. Mao, Y. Chen, D. Liu, J. Zhang, L. Xie, Solvatochromic effect on the photoluminescence of MoS_2 monolayers, Small, 9 (2013) 1312-1315.
[28] Y.H. Lee, L. Yu, H. Wang, W. Fang, X. Ling, Y. Shi, C.T. Lin, J.K. Huang, M.T. Chang, C.S. Chang, M. Dresselhaus, T. Palacios, L.J. Li, J. Kong, Synthesis and transfer of single-layer transition metal disulfides on diverse surfaces, Nano Lett. , 13 (2013) 1852-1857.
[29] L. Sun, X. Yan, J. Zheng, H. Yu, Z. Lu, S.P. Gao, L. Liu, X. Pan, D. Wang, Z. Wang, P. Wang, L. Jiao, Layer-Dependent Chemically Induced Phase Transition of Two-Dimensional MoS_2, Nano Lett. , 18 (2018) 3435-3440.

[30] Y. Li, X. Li, T. Yu, G. Yang, H. Chen, C. Zhang, Q. Feng, J. Ma, W. Liu, H. Xu, Y. Liu, X. Liu, Accurate identification of layer number for few-layer WS_2 and WSe_2 via spectroscopic study, Nanotechnology, 29 (2018) 124001.
[31] P. Hu, J. Ye, X. He, K. Du, K.K. Zhang, X. Wang, Q. Xiong, Z. Liu, H. Jiang, C. Kloc, Control of Radiative Exciton Recombination by Charge Transfer Induced Surface Dipoles in MoS_2 and WS_2 Monolayers, Sci Rep, 6 (2016) 24105.
[32] M. O'Brien, N. McEvoy, D. Hanlon, T. Hallam, J.N. Coleman, G.S. Duesberg, Mapping of Low-Frequency Raman Modes in CVD-Grown Transition Metal Dichalcogenides: Layer Number, Stacking Orientation and Resonant Effects, Sci Rep, 6 (2016) 19476.
[33] S. Kim, K. Kim, J.-U. Lee, H. Cheong, Excitonic resonance effects and Davydov splitting in circularly polarized Raman spectra of few-layer WSe_2, 2D Materials, 4 (2017) 045002.